Interlocking Inorganic Screw Helices: Synthesis, Structure, and Magnetism of the Novel Framework Uranium Orthothiophoshates $A_{11}U_7(PS_4)_{13}$ (A = K, Rb)

Christine Gieck and Wolfgang Tremel*[a]

Abstract: The novel quaternary uranium thiophosphate $K_{11}U_7(PS_4)_{13}$ has been synthesized by reacting uranium metal, K_2S, S, and P_2S_5 at 700 °C in an evacuated silica tube. The crystal structure was determined by single crystal X-ray diffraction techniques. $K_{11}U_7(PS_4)_{13}$ crystallizes in the tetragonal space group $I\bar{4}2d$ ($a = 32.048(2)$ Å, $c = 17.321(1)$ Å, $Z = 8$). The structure contains a tunnel framework composed of eight interlocking uranium $U_7(PS_4)_{13}$ screw helices, with alkali metal cations residing inside the framework channels. The uranium atoms are coordinated in a bi- or tricapped trigonal prismatic fashion. The screw helices are built up from uranium atoms interconnected by PS_4 tetrahedral units. Magnetic susceptibility measurements indicate modified Curie–Weiss-type behavior between 300 and 70 K, with an effective magnetic moment of 2.54 μ_B per U atom at room temperature and $C = 3.78$, $\theta = -14.54$, $\chi_0 = 0.01$. The isostructural compound $Rb_{11}U_7(PS_4)_{13}$ ($a = 32.1641(11)$ Å, $c = 17.7244(9)$ Å, $Z = 8$) was prepared by heating a mixture of the formal composition UPS_5 in eutectic LiCl/RbCl melts at 700 °C.

Keywords: chalcogens · magnetic properties · solid-state structures · thiophosphates · uranium

Introduction

Orthothiophosphates are built up from PS_4 groups that are separated and charge balanced by main group elements, transition metals, or f block elements. Formally, thiophosphates in general represent higher homologues of oxophosphates. Although there are some similarities originating from the underlying pattern of tetrahedral building blocks, the chemistry of phosphates and thiophosphates is very different and their overlap therefore limited. As for most other chalcogenides this is caused by the stronger covalency of the P–S bonds relative to the P–O bonds and the redox properties of the S component. Main group and transition metal thiophosphates have been known for more than hundred years.[1] Surveys by Rouxel,[2] Brec,[3] and Kanatzidis,[4, 5] show a remarkable variety of structures. As in any branch of chemistry where complex structures have to be analyzed, a simple strategy can be used: one decomposes the structures into elementary building blocks, and then tries to identify and explore the matching rules according to which these blocks must be reassembled to yield the considered structure. In chalcophosphate chemistry (or chalcometalate chemistry in general), a rich structural chemistry emerges from the combination of isolated or condensed P_mS_n motifs and a large variety of metal chalcogenide units. With phosphorus and transition metals, chalcogens generally form low-dimensional compounds, the thiophosphates MPS_3 (e.g., M = Al, Mn, Fe, Co, Ni, Zn) being especially well-characterized representatives of this class of materials.[3]

During the past decade many studies have focussed on the chalcophilic late transition metal derivatives, whose structures contain metal atoms mostly in tetrahedral, square-planar, or octahedral coordination. Much less effort has been devoted to the chalcophosphates of the oxophilic early transition metals.[6–15] Many of these larger metal cations are observed in seven, eight, or higher coordinate environments. These high and variable coordination numbers of the early transition metals,[7–8, 13–15] lanthanides,[16–25] or actinides[26–30] combined with the condensation equilibria of chalcophosphates[2, 5] may lead to structural arrangements of astounding complexity, as the following examples indicate.

Many compounds obtained from the ternary system M-P-S (M = Group 5 metal) contain the bicapped biprismatic M_2S_{12} building unit.[2] Interestingly, the channels of some of the resulting three-dimensional framework structures (e.g., $TaPS_6$[7]) may be filled with chalcogen chains.[31] The structures of several other thiophosphates (e.g., $ATi_2(PS_4)_3$; A = Li, Na[32–34]) are composed of interwoven networks whose channels are filled with alkali metal cations.[32] Finally the structure of UP_4S_{12} is based on three interwoven polymeric diamond-type $U(P_2S_6)_2$ frameworks.[30]

[a] Prof. Dr. W. Tremel, C. Gieck
Institut für Anorganische Chemie und Analytische Chemie
der Johannes Gutenberg-Universität
Duesbergweg 10-14, 55099 Mainz (Germany)
Fax: (+49) 6131-39-22284
E-mail: tremel@mail.uni-mainz.de

  0947-6539/02/0813-2980 $ 17.50+.50/0

The coordination preferences of the metal components seem to be important factors, which determine the structure (and properties) of thiophosphates. Therefore we were interested in introducing transition metals with high coordination numbers, that is, Group 4 metals, lanthanides, or actinides, to preclude the formation of octahedrally coordinated metal centers. The example UP_4S_{12}[30] revealed that the coordination mode of the metal atom combined with the connectivity mode and size of the "linear" (rodlike) $P_2S_6^{2-}$ ligand may lead to the formation of complex network structures. Herein we show that the nonlinear PS_4^{3-} ligand can lead to the formation of metal thiophosphates with helical structure elements.

Results and Discussion

The new compound $K_{11}U_7(PS_4)_{13}$ was obtained by reaction of uranium metal with a thiophosphate melt at 700 °C. $Rb_{11}U_7(PS_4)_{13}$ was prepared by heating a mixture of the formal composition UPS_5 in an eutectic RbCl/LiCl flux at 700 °C. A perspective view of the crystal structure of $A_{11}U_7(PS_4)_{13}$ (A = K, Rb) along the crystallographic *c* axis is shown in Figure 1 (top). Selected interatomic bond lengths are compiled in Tables 1 and 2. Principle features of this novel structure type are spiral $U_7(PS_4)_{13}$ chains extending along the view direction. One of these chains is shown in a view along the helix axis in Figure 1 (bottom). Four chains are marked by circles in Figure 1 (top). Each of the individual chains is cross-linked to five neighboring chains by two *exo*-PS_4 groups per linkage. The connectivity of the covalently linked uranium thiophosphate framework generates different types of cavities and a topologically unusual array of tunnels that contain the A^+ counterions. The coordination geometries of the A^+ counterions are quite irregular with coordination numbers between six and eight with K–S separations varying between 3.160(9) Å and 3.739(8) Å and Rb–S distances between 3.247(7) Å and 3.980(6) Å.

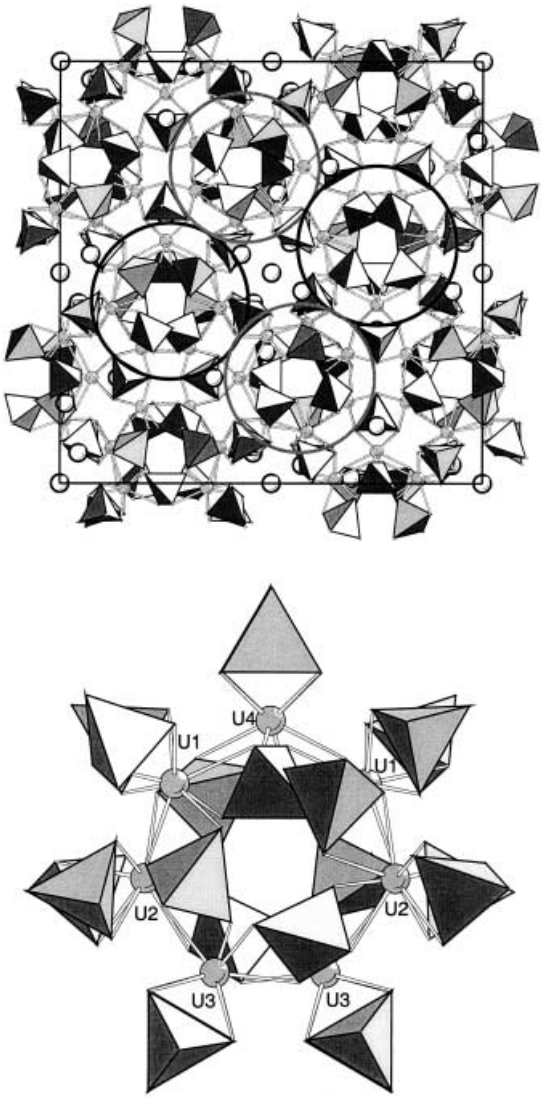

Figure 1. Top: View of the unit cell down the *c* axis (grey circles: U, white circles: K) illustrating the positions of the alkali cations in the structure channels; large grey and black circles indicate the opposite helicity of the chains. Bottom: Enlarged view of the circled fragment illustrating the connectivity of the uranium centers by the PS_4 units.

Abstract in German: *Das neuartige quaternäre Uranthiophosphat $K_{11}U_7(PS_4)_{13}$ wurde durch Erhitzen von elementarem Uran, K_2S, Schwefel und P_2S_5 auf 700° in evakuierten Quarzglasampullen dargestellt. Die Kristallstruktur wurde mittels Röntgenstrukturanalyse an Einkristallen bestimmt. $K_{11}U_7(PS_4)_{13}$ kristallisiert in der tetragonalen Raumgruppe $I\bar{4}2d$ ($a = 32.048(2)$ Å, $c = 17.321(1)$ Å, $Z = 8$). Die Struktur besteht aus einem von drei Kanälen unterschiedlichen Durchmessers durchzogenen Gerüst von acht miteinander verknüpften $U_7(PS_4)_{13}$-Helices. Die Kationen sind in die Kanäle des Strukturgerüsts eingebaut. Die Uranatome treten in zwei- bzw. dreifach überkappt trigonal-prismatischer Koordination auf, wobei jedes Uranatom von vier PS_4-Gruppen umgeben ist. Die Ergebnisse magnetischer Suszeptibilitätsmessungen an $K_{11}U_7(PS_4)_{13}$ zeigen im Bereich von 300 – 70 K ein modifiziertes Curie-Weiss-Verhalten, mit $C = 3.78$, $\theta = -14.54$ K, $\chi_0 = 0.01$ emu mol^{-1}; das effektive magnetische Moment bei Raumtemperatur beträgt 2.54 μ_B pro U-Atom. Das isotrukturelle $Rb_{11}U_7(PS_4)_{13}$ ($a = 32.1641(11)$ Å, $c = 17.7244(9)$ Å, $Z = 8$) konnte durch Erhitzen einer Schmelze der formalen Zusammensetzung UPS_5 in einer eutektischen LiCl/RbCl Mischung bei 700 °C synthetisiert werden.*

Metal coordination: As in several other uranium chalcogenides the framework structure of $A_{11}U_7(PS_4)_{13}$ (A = K, Rb) is based on bicapped trigonal prismatic US_8 units, US_9 tricapped trigonal prisms and PS_4 tetrahedra. The U coordination is illustrated in Figure 2, which shows a fragment of the structure about U4 that is situated on a crystallographic twofold axis. In the capped prisms, the U atoms have eight S neighbors with distances ranging from 2.771 Å to 2.941 Å; U2 acquires an additional S neighbor at a slightly larger distance of 3.110(5) Å; this leads to a tricapped trigonal prismatic coordination geometry that is uncommon for uranium chalcogenides.[29] A number of uranium chalcogenides, such as $Cu_2U_3S_7$,[35] US_3,[36] or MUS_3(M = Ru, Rh),[37] exhibit bicap-

Table 1. Selected bond lengths [Å] for $K_{11}U_7(PS_4)_{13}$.

U1–S1	2.822(5)	U2–S15	2.839(4)
U1–S4	2.889(5)	U2–S16	2.867(4)
U1–S5	2.892(4)	U2–P1	3.337(5)
U1–S6	2.834(4)	U3–S19	2.722(4)
U1–S7	2.822(5)	U3–S20	2.891(4)
U1–S9	2.803(4)	U3–S20 (2×)	2.916(4)
U1–S17	2.753(5)	U3–S21	2.751(5)
U1–S22	2.775(5)	U3–S23	2.798(4)
U2–S4	3.015(5)	U3–S24	2.933(5)
U2–S7	3.110(5)	U3–S25	2.813(5)
U2–S9	2.916(5)	U4–S3 (2×)	2.803(5)
U2–S10	2.828(5)	U4–S24 (2×)	2.942(4)
U2–S11	2.855(4)	U4–S25 (2×)	2.847(5)
U2–S12	2.851(4)	U4–S26 (2×)	2.769(4)
U2–S14	2.821(4)		
P1–S2	1.930(8)	P4–S6	2.007(6)
P1–S4	2.110(7)	P4–S21	2.066(6)
P1–S7	2.226(9)	P4–S22	2.005(6)
P1–S11	2.032(7)	P4–S23	2.040(6)
P2–S1	2.057(7)	P5–S13	1.936(7)
P2–S8	1.984(7)	P5–S20	2.061(6)
P2–S9	2.052(7)	P5–S24	2.084(6)
P2–S10	2.047(7)	P5–S25	2.032(7)
P3–S14	2.044(6)	P6–S3	2.045(6)
P3–S15	2.015(6)	P6–S12	2.031(6)
P3–S18	2.046(6)	P6–S16	2.024(6)
P3–S19	2.069(6)	P6–S26	2.040(6)
		P7–S5 (2×)	2.028(6)
		P7–S17 (2×)	2.029(6)

Table 2. Selected bond lengths [Å] for $Rb_{11}U_7(PS_4)_{13}$.

U1–S1	2.801(6)	U2–S15	2.850(5)
U1–S4	2.878(5)	U2–S16	2.861(5)
U1–S5	2.878(6)	U2–P1	3.312(6)
U1–S6	2.866(6)	U3–S19	2.727(5)
U1–S7	2.846(5)	U3–S20	2.891(5)
U1–S9	2.809(5)	U3–S20 (2×)	2.914(5)
U1–S17	2.771(6)	U3–S21	2.763(6)
U1–S22	2.787(5)	U3–S23	2.780(5)
U2–S4	3.054(5)	U3–S24	2.939(5)
U2–S6	3.117(6)	U3–S25	2.825(6)
U2–S9	2.919(5)	U4–S3 (2×)	2.803(5)
U2–S10	2.828(5)	U4–S24 (2×)	2.942(5)
U2–S11	2.863(5)	U4–S25 (2×)	2.866(6)
U2–S12	2.848(5)	U4–S26 (2×)	2.755(5)
U2–S14	2.840(5)		
P1–S2	1.956(8)	P4–S6	2.046(8)
P1–S4	2.100(8)	P4–S21	2.040(8)
P1–S6	2.092(8)	P4–S22	2.007(8)
P1–S11	2.028(8)	P4–S23	2.056(8)
P2–S1	2.051(8)	P5–S13	1.948(8)
P2–S8	1.968(8)	P5–S20	2.079(7)
P2–S9	2.081(8)	P5–S24	2.068(8)
P2–S10	2.065(7)	P5–S25	2.055(8)
P3–S14	2.026(8)	P6–S3	2.047(7)
P3–S15	2.015(7)	P6–S12	2.025(8)
P3–S18	2.045(8)	P6–S16	2.005(7)
P3–S19	2.071(8)	P6–S26	2.055(7)
		P7–S5 (2×)	2.031(7)
		P7–S17 (2×)	2.034(8)

ped trigonal prismatic geometry; square bipyramidal S coordination has been observed in US_2,[38] or ternary thiophosphates, such as UP_2S_6[26] UP_2S_7,[39] or $U(P_2S_6)_2$.[30] The average U–S distance of 2.873 Å indicates uranium to be in the tetravalent state[40] and compares well with the

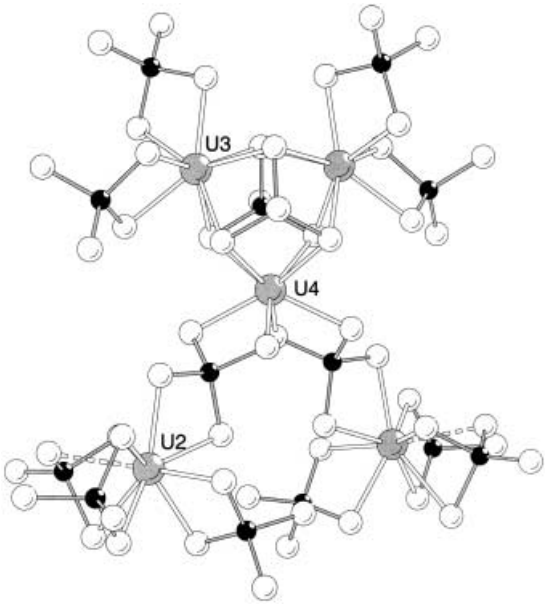

Figure 2. Coordination of the uranium atoms with atomic labeling scheme.

U–S distances observed in US_2[38] or other U chalcogenides.[26, 30, 35–37, 39] The PS_4 tetrahedra in $K_{11}U_7(PS_4)_{13}$ are slightly distorted; as expected, the P–S distances to the doubly metal-bridging S atoms ($d_{P-S} = 2.095$ Å) are slightly longer than those with a single metal bond ($d_{P-S} = 2.034$ Å) or terminal S atoms ($d_{P-S} = 1.941$ Å). We note that some of the terminal P–S distances are remarkably short.

Helix formation: In Figure 3 prisms made up of the S atoms of four PS_4^{3-} anions surrounding U3 are depicted; two S atoms of two of the PS_4^{3-} anions form one rectangular face of the prism, while two S atoms of the remaining two PS_4^{3-} anions occupy the remaining corners of the prism as well as capping the other two rectangular faces. It should be noted that the two capping PS_4^{3-} anions may have different (right/left) orientation with respect to the prism, that is, because of the chelating nature of the PS_4^{3-} ligand the $[U(PS_4)_4]^{8-}$ unit is a chiral center with one of the capping PS_4^{3-} groups pointing "up" and the other one pointing "down". The upper corner of each unit is condensed with the lower corner of an adjacent unit. As the doubly bidentate PS_4^{3-} groups provide an approximately linear linkage of the U centers and the "pitch angle" of the chains defined by the P-U-P vectors is slightly larger than 90°, a helix is formed that ideally should have four (or a multiple of four) prismatic units per repeat distance spiraling around the twofold screw axes parallel to the *c* axis. This can been seen from Figure 3. However, as the helix pitch angle is $> 90°$, the unit cell of the title compound contains only seven $[U(PS_4)_4]^{8-}$ prism units per unit cell. This is illustrated by a simplified view of the U–P backbone of the spiral chains (with the S atoms omitted) in Figure 4. The deviations of the P-U-P (91.2–93.7°) and U-P-U (168.0–177.4°) angles from their idealized values of 90° and 180°, respectively, lead to an irregular pitch of the helix.

As for any other helix, the "prism helix" in the structure of the title compound may be either left or right handed. In this structure spiral chains around adjacent axes, which are cross-

0947-6539/02/0813-2982 $ 17.50+.50/0 *Chem. Eur. J.* **2002**, *8*, No. 13

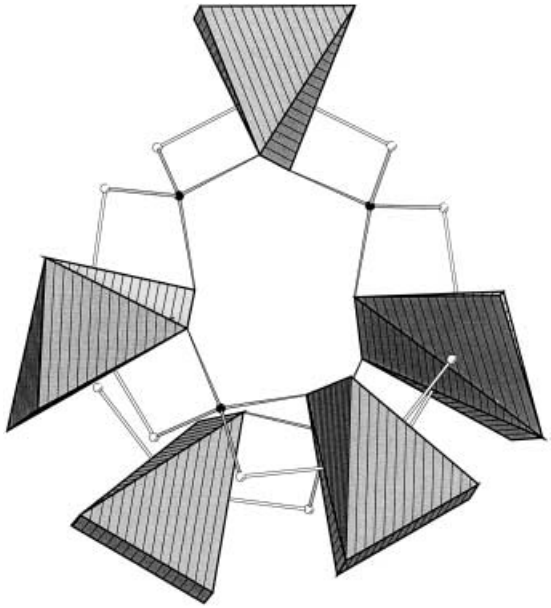

Figure 3. Schematic polyhedral representation of the $[U_7(PS_4)_{13}]^{11-}$ helix in $K_{11}U(PS_4)_{13}$.

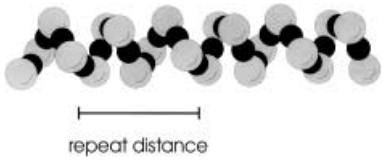

Figure 4. CPK representation of the backbone of the $[U_7(PS_4)_{13}]^{11-}$ helix chain in $K_{11}U_7(PS_4)_{13}$ (S atoms omitted for clarity).

linked by common PS_4^{3-} groups (two PS_4^{3-} groups per linkage), have a different sense of rotation as indicated by the black and grey circles in Figure 1 (top).

Framework channels: The helix formation and the cross-linking of the helices are illustrated in Figure 1 (top). Four helices centered about the fourfold inversion axes (along 0, 0, z and ½, ½, z) form a set of large tunnels with a diameter of approximately 5 Å that contain the majority of the K^+ ions. A second set of smaller tunnels is formed around the twofold screw axes along (¼, ¼, z) by four helices linked by PS_4^{3-} groups. These triply-connecting tetrahedra are situated above or below a second set of K^+ ions. The remaining cations are located between the PS_4^{3-} groups spiraling along [0 0 1] within the helices. The cation sizes (K^+: 1.39 Å, Rb^+: 1.60 Å)[41] are small compared to the diameter of the large tunnel, and one of the seven crystallographically independent cations (K7) seems to "rattle" within the channels, as indicated by its disorder and the large and strongly anisotropic displacement parameters. This is also the case for the larger Rb^+ ion in the isostructural $Rb_{11}U_7(PS_4)_{13}$. The large tunnel diameter, the high thermal parameters for the A^+ ions inside the tunnel, the existence of the isostructural compounds $A_{11}U_7(PS_4)_{13}$ (A = K, Rb), and the fractional distribution of the A^+ ions over several lattice sites indicate that $A_{11}U_7(PS_4)_{13}$ (A = alkali metal) may act as host for ion exchange. Based on these observations, we have probed the potential ion-exchange properties for $K_{11}U_7(PS_4)_{13}$ by means of solid–solid ion exchange with iodides,[42, 43] a synthetic approach which has been used for ion exchange in a number of open-framework compounds. More detailed results will be given in a subsequent report.

Vibrational and spectral properties: The IR spectroscopic data for $K_{11}U_7((PS_4)_{13}$ show absorptions at 610 (ν_3), 420 (ν_1), 220 (ν_4) and 170 cm^{-1} (ν_2). Absorbances in a related spectral range have been observed for thiophosphates such as $NaPS_4 \times 8H_2O$[51] or $KPdPS_4$.[52] According to the results of the X-ray structure determination the spectroscopically relevant unit is the PS_4^{3-} anion. For this tetrahedral species four Raman ($\nu_1-\nu_4$) and two IR (ν_3 and ν_4) bands are expected.[53] Due to the symmetry reduction in the structure of the title compound, all vibrational bands are visible in the IR spectrum. Neglecting the high- and low-frequency parts of the spectrum (combinations and lattice + deformation modes), the vibrational spectrum of $K_{11}U_7(PS_4)_{13}$ is essentially a juxtaposition of bands characteristic of the US_8 unit (outside the detection range; U–S stretching modes are expected in the frequency range below 140 cm^{-1}) and of those of the PS_4^{3-} anion. This result confirms the proposed description of the crystal structure in terms of ionic fragments, but also the predominance of nearest neighbor interactions of covalent character.

The optical properties of $K_{11}U_7(PS_4)_{13}$ were determined by studying the UV-visible/near-mid IR diffuse reflectance spectrum, which reveals well-defined broad peaks at ≈5000 (0.61), ≈7100 (0.87), ≈8300 (1.02), ≈9650 (1.14), ≈11700 (1.44), and ≈12500 cm^{-1} (1.54 eV). Based on the oxidation state formalism, a $5f^2$ configuration and semiconducting behavior may be expected. Assuming a $^3H_4$ ground state, other triplet terms arising from this configuration are ^3F and ^3P. Based on their position and spectral width, the absorptions are assigned to f–f or d–d transitions.[54] $K_2UP_3Se_9$, which contains U^{4+}, displays absorptions at 3725 and 5856 cm^{-1}.[27]

Magnetic properties: The oxidation states of the uranium atoms may be deduced from simple charge balance considerations. The electronic structure of the title compound may easily be understood by electron counting and assigning formal oxidation states according to the formula $[K^+]_{11}[(U^{4+})_7(PS_4^{3-})_{13}]$.

Magnetic measurements between 4 and 300 K were made on polycrystalline powdered samples of $K_{11}U_7(PS_4)_{13}$ by using a Foner vibrating sample magnetometer. Figure 5 shows the thermal variation of the inverse susceptibility and the effective magnetic moment. The $1/\chi$ versus T curve shows a distinct minimum at approximately 60 K characteristic of an antiferromagnetic transition. In the paramagnetic region, the thermal variation of χ shows some curvature towards the temperature axis. A curve fitting using the modified Curie–Weiss law $\chi = C/(T-\theta) + \chi_0$ in the temperature range 70–300 K led to the values $C = 3.78$, $\theta = -14.54$ K, $\chi_0 = 0.01$ for the Curie constant, the paramagnetic Neél temperature, and magnetic susceptibility, respectively, and to an effective magnetic moment of 2.54 μ_B per U atom. The value for the

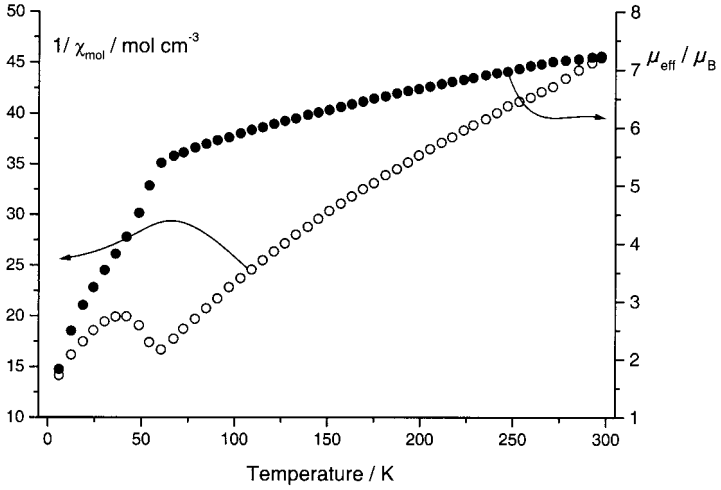

Figure 5. Thermal variation of the inverse molar susceptibility (filled circles) and the effective magnetic moment (open circles) for $K_{11}U_7(PS_4)_{13}$. The data have been corrected for core diamagnetism.

effective paramagnetic moment of uranium is significantly lower than the theoretical value for a U^{4+} free ion of 3.58 μ_B ($^3H_4$ ground term) and is also lower than that for a totally quenched orbital moment (2.83 μ_B).[47–49] The large reduction of the effective magnetic moment probably results from crystal field interactions as observed and theoretically confirmed for UP_4S_{12} from calculations based on the angular overlap model.[50] The results of calculations for UP_4S_{12} confirm the presence of a non-magnetic ground state, and we assume a related behavior in the present case.

Conclusion

The reaction of K_2S, uranium, P_2S_5, and sulfur leads to the formation of a new framework compound $K_{11}U_7(PS_4)_{13}$, whose tunnel structure is made of interlocked helical chains which are themselves built from complex polyhedral interconnections. The helix formation in turn is related to the bicapped trigonal prismatic coordination of the uranium centers. A comparison with other uranium ortho- and dithiophosphates indicates that square-antiprismatic coordination of the metal atoms is compatible with a pseudotetrahedral connectivity within the framework.[30, 51] Based on the results from systematic studies of the ternary system U-P-S and structural considerations, we assume that several other uranium thiophosphates with low density may occur. This would deserve further exploitation of the A-U-P-S system.

The synthesis of interpenetrating framework materials, such as $U(P_2S_6)_2$,[30] or open framework compounds, such as $CsLiU(PS_4)_2$[51] and $K_{11}U_7(PS_4)_{13}$, suggest several areas of additional research. 1) These compounds may be derivatized by "soft chemistry" methods such as ion exchange. 2) The ion transport within the channels is worthwhile to pursue. 3) The compound $Rb_{11}U_7(PS_4)_{13}$ seems to be metastable because it could not be prepared by high-temperature solid-state or (poly)thiophosphate flux reactions. 4) Rare earth metals are widely used to prepare magnetic materials with interesting bulk properties, which are determined by the anisotropy of the ground state of the 4f ions and the nature of the lanthanide–lanthanide and/or lanthanide–transition metal interactions. It might be worthwhile to pursue to interplay of ligand field effects and/or magnetic interactions between the lanthanide/actinide atoms. Although magnetically interacting rare earth centers with organic radicals or Schiff base complexes have been described, magnetic interactions between actinide centers mediated by the σ-bonded (PS_4^{3-}) ligands would be unusual.

Experimental Section

Materials: The starting materials were uranium metal powder (Kristallhandel Kelpin, 99.9% purity), P_2S_5 (Aldrich, 99% purity), K_2S, S powder (Riedel, 99.999%), RbCl (Alfa Aesar, 99.8%) and LiCl (Alfa Aesar, 99.996%). All starting compounds and products were examined by X-ray powder diffraction, by means of a Siemens D5000 diffractometer with a $Cu_{K\alpha}$ source.

Potassium sulfide (K_2S): K_2S was made following the procedure:[52] Potassium (3.9 g, 100 mmol) was placed under an Ar atmosphere on the glas frit of a Schlenk tube. The tube was cooled to $-78\,^\circ C$ with a dry ice/acetone bath and NH_3 (ca. 30 mL) was condensed into the tube. After the metal was dissolved, elemental sulfur (1.6 g) was placed on the frit and dissolved by condensing a second portion of NH_3 onto the reactants. The resulting dark blue solution was stirred and the NH_3 was allowed to evaporate. A third portion of NH_3 was condensed on the product to ensure that the reaction was complete. After evaporating the NH_3 a light yellow product was obtained. The yellow color indicated contamination with K_2S_2 (pure K_2S should be white). Samples with a stronger yellow tone had to be subjected to an additional reduction with K. All substances were handled under argon atmosphere in a stainless steel glove box.

$K_{11}U_7(PS_4)_{13}$: Uranium (0.254 g, 1.06 mmol), P_2S_5 (0.119 g, 0.53 mmol), K_2S (0.059 g, 0.53 mmol), and sulfur (0.068 g, 2.12 mmol) were sealed under vacuum ($<10^{-5}$ bar) in a silica tube with 8 mm outer diameter and placed in a programmable tube furnace. The tube was heated up to 130 °C over a period of 10 h and kept at this temperature for 24 h. Subsequently, it was heated up to 700 °C at a rate of 20 °C min^{-1} and maintained at that temperature for 50 h. Finally, the sample was cooled down to room temperature at a rate of 0.5 °C min^{-1}. The yield of the black crystalline material was quantitative based on the initial metal content as judged by X-ray powder diffraction. Slight impurities of soluble thiophosphates (with presumably discrete anionic structures) were removed by washing with dry ethanol. A semiquantitative microprobe analysis (EDAX) indicated to presence of K, U, P, and S in an approximate atomic ratio of 2:1:2:4. According to the X-ray powder diffractometrical results the sample was a single phase.

$Rb_{11}U_7(PS_4)_{13}$: A sample with the formal composition UPS_5 (0.250 g, 3.7 μmol) was sealed with a eutectic LiCl/RbCl mixture (1.5 g) under vacuum in a quartz ampoule with an outer diameter of 8 mm. The sample was placed in a programmable tube furnace and heated from room temperature up to 700 °C at a rate of 10 °C h^{-1}, kept at that temperature for 60 h and cooled down to room temperature at a rate of 0.5 °C min^{-1}. The reaction product contained dark red needle-shaped crystals embedded in a LiCl/RbCl matrix. The LiCl/RbCl mixture could be removed by treating the product with dry methanol. The yield of the black crystalline material was approximately 90% based on the initial metal content as judged by X-ray powder diffraction. A semiquantitative microprobe analysis (EDAX) indicated to presence of Rb, U, P, and S in an approximate atomic ratio of 2:1:2:4. Attempts to prepare $Rb_{11}U_7(PS_4)_{13}$ from high temperature reactions or from thiophosphate fluxes did not lead to the desired results. $Rb_{11}U_7(PS_4)_{13}$ could, however, be obtained by treating a sample of the formal composition $CsU_2(PS_4)_5$ at 700 °C in a LiCl/RbCl mixture. In this case, small amounts of another phase with the composition $Li_3Rb_6U_3P_5S_{23}$ were formed as black platelike crystals.[53]

Structure determinations: Single crystals of $K_{11}U_7(PS_4)_{13}$ and $Rb_{11}U_7(PS_4)_{13}$ were selected from the reaction mixtures, embedded in a thin film of epoxy

  0947-6539/02/0813-2984 $ 17.50+.50/0 *Chem. Eur. J.* **2002**, *8*, No. 13

glue and fixed at the tip of a glass fiber on a Bruker SMART CCD diffractometer[54] equipped with a monochromated $Mo_{K\alpha}$ source ($\lambda = 0.71073$ Å) and a graphite monochromator. Cell parameters were initially calculated from reflections taken from approximately 30 frames. The final lattice parameters were calculated from all reflections observed in the actual data collection. A summary of details concerning the data collections, structure solutions and refinements is given in Table 3. The collected data were processed by using the SAINT[55] program and corrected for absorption by using SADABS.[56] The systematic absence conditions ($hkl, h + k + l = 2n$; $hk0, h + k = 2n$) were characteristic for the tetragonal space group $I\bar{4}2d$ (No. 122), and the refinement results proved this choice to be correct. The structures were solved by direct methods with SHELXS-86[57] and refined in full-matrix least-squares with SHELXL-97.[58] The final refinement was carried out on F_o^2. Atomic scattering factors for spherical neutral free atoms were taken from standard sources and anomalous dispersion corrections were applied.[59] From the final refinement cycle the compositions of the crystals used are $K_{11}U_4(PS_4)_{13}$ and $Rb_{11}U_4(PS_4)_{13}$. Analysis of F_o^2 versus F_c^2 as a function of F_o^2, setting angles, or Miller indices revealed no unusual trends. Calculations performed at an intermediate stage in which the relative positional occupancies were refined, did not indicate any nonstoichiometry. The final atomic parameters are listed in Tables 4 and 5. The molecular graphics were produced with the Diamond plot program.[60] Further details on the crystal structure investigation(s) may be obtained from the Fachinformationszentrum Karlsruhe, 76344 Eggenstein-Leopoldshafen, Germany (fax: (+49) 7247-808-666; e-mail: crysdata@fiz-karlsruhe.de), on quoting the depository numbers CSD-412201 and CSD-412202.

Semiquantitative microprobe analysis: Semiquantitative microprobe analysis was performed in a Zeiss DSM 962/Philipps PSEM 500 scanning electron microscope equipped with a KEVEX energy dispersive spectroscopy detector. Data acquisition was performed with an accelerating voltage of 20 kV and a 1 min accumulation time.

FT-IR spectra: FT-IR spectra were recorded on solid samples in a CsI matrix. The samples were ground with dry CsI into a fine powder and pressed into transparent pellets. The spectra were recorded in the far-IR region (700–200 cm^{-1}, $\approx 5\ cm^{-1}$ resolution) with a FT-IR spectrometer (2030 Galaxy-FT-IR, Mattson Instruments) equipped with a TGS/PE detector and a silicon beam splitter.

Table 3. Crystal data and structure refinement for $K_{11}U_7(PS_4)_{13}$ and $Rb_{11}P_{13}S_{52}U_7$.

	$K_{11}P_{13}S_{52}U_7$	$Rb_{11}P_{13}S_{52}U_7$
formula weight	4166.04	4676.11
crystal system	tetragonal	tetragonal
space group	$I\bar{4}2d$	$I\bar{4}2d$
a [Å]	32.048(2)	32.164(1)
c [Å]	17.321(1) Å	17.724(1)
V [Å^3]	17789.9(18)	18336.4(13)
Z	8	8
ρ_{calcd} [g cm^{-3}]	3.111	3.388
crystal size [mm]	0.2 × 0.2 × 0.1	0.2 × 0.2 × 0.1
T [K]	203	183(2)
μ ($Mo_{K\alpha}$) [mm^{-1}]	14.689	19.554
θ range [°]	2.01–28.29	2.00–28.31
index ranges	$-42 \le h \le 42$	$-42 \le h \le 37$
	$-42 \le k \le 42$	$-38 \le k \le 42$
	$-22 \le l \le 23$	$-17 \le l \le 23$
measured reflections	81364	79281
independent reflections	11046	11401
observed reflections [$I > 2\sigma(I)$]	6272	7018
R_{int}	0.1890	0.2001
parameters	379	378
goodness-of-fit on F^2	0.845	0.963
Flack parameter	0.024(7)	–
R values [$I > 2\sigma(I)$]	$R1 = 0.0535$,	$R1 = 0.0545$,
	$wR2 = 0.0799$	$wR2 = 0.1105$
R values (all data)	$R1 = 0.1189$,	$R1 = 0.1288$,
	$wR2 = 0.0911$	$wR2 = 0.1348$
residual electron density [e Å^{-3}]	3.060/−1.245	3.348/−3.547

Table 4. Atomic coordinates ($\times 10^4$) and equivalent isotropic displacement parameters (Å$^2 \times 10^3$) for $K_{11}U_7(PS_4)_{13}$. U(eq) is defined as one third of the trace of the orthogonalized U_{ij} tensor.

	x	y	z	U(eq)
U1	119(1)	1519(1)	2118(1)	26(1)
U2	1222(1)	844(1)	2387(1)	20(1)
U3	3065(1)	1808(1)	1252(1)	21(1)
U4	4238(1)	2500	1250	21(1)
S1	17(2)	976(2)	849(3)	39(1)
S2	58(2)	945(2)	4525(3)	61(2)
S3	267(1)	2633(1)	4940(3)	30(1)
S4	305(2)	682(2)	2637(3)	36(1)
S5	501(1)	2664(1)	331(3)	29(1)
S6	717(1)	6232(2)	347(3)	32(1)
S7	728(2)	1520(2)	3295(3)	34(1)
S8	756(2)	3890(2)	2999(3)	51(2)
S9	877(1)	1457(1)	1318(3)	30(1)
S10	922(2)	468(2)	1018(3)	32(1)
S11	1025(1)	612(1)	3936(2)	30(1)
S12	1344(1)	5034(1)	247(3)	24(1)
S13	1573(2)	2597(2)	3621(3)	58(2)
S14	1676(1)	1585(1)	2649(3)	27(1)
S15	1855(1)	926(1)	1251(3)	25(1)
S16	1959(1)	592(1)	3200(3)	25(1)
S17	2010(2)	4771(2)	3483(3)	49(2)
S18	2197(1)	1906(1)	1049(3)	30(1)
S19	2668(1)	1317(1)	2304(3)	28(1)
S20	2871(1)	2494(1)	229(2)	24(1)
S21	2900(2)	1289(2)	23(3)	35(1)
S22	3010(2)	335(1)	667(3)	36(1)
S23	3598(1)	1121(1)	1378(3)	25(1)
S24	3741(1)	3002(1)	164(3)	26(1)
S25	3743(2)	1985(2)	273(3)	36(1)
S26	4630(1)	1735(1)	1412(3)	28(1)
P1	479(2)	916(2)	3730(3)	58(2)
P2	645(2)	999(2)	609(3)	28(1)
P3	2092(1)	1426(1)	1803(3)	24(1)
P4	3326(1)	859(1)	430(3)	23(1)
P5	3454(1)	2533(2)	2769(3)	28(1)
P6	4984(1)	1851(1)	457(3)	21(1)
P7	145(2)	2500	1250	22(1)
K1	124(2)	3113(2)	3210(3)	68(2)
K2	1765(2)	3727(2)	3108(3)	75(2)
K3	3125(1)	423(1)	2475(2)	42(1)
K4	4565(1)	719(1)	1172(3)	54(1)
K5	1365(2)	2500	1250	85(3)
K6	6965(2)	2500	1250	42(2)
K7a[a]	102(4)	−570(4)	1273(4)	95(5)
K7b[a]	−102(4)	570(4)	1273(4)	98(5)

[a] Occupancy 50%.

Optical spectroscopy: Optical diffuse reflectance measurements were made at room temperature with a Varian CARY5 double-beam, double-monochromator spectrophotometer operating in the 200–2000 nm region. The instrument was equipped with an integrating sphere and controlled by a personal computer. The measurement of diffuse reflectivity may be used to determine values for the optical band gap, which are in reasonable agreement with those obtained from single-crystal absorption measurements. $BaSO_4$ was used as reference material (100% reflectivity assumed).[61–63]

Magnetic susceptibility measurements: Variable-temperature magnetic susceptibility data were collected for a sample of $K_{11}U_7(PS_4)_{13}$ (79 mg) with a vibrating sample magnetometer (Foner-magnetometer, Princeton Applied Research), which was operated between 0.2 and 1 T. The instrument was calibrated with $Hg[Co(NCS)_4]$. Measurements at different field strengths confirmed that ferromagnetic impurities were absent. The diamagnetic correction was estimated from Pascal's constants to be -310×10^{-6} cm^3 mol^{-1}.[64]

Table 5. Atomic coordinates ($\times 10^4$) and equivalent isotropic displacement parameters ($Å^2 \times 10^3$) for $Rb_{11}U_7(PS_4)_{13}$. U(eq) is defined as one third of the trace of the orthogonalized U_{ij} tensor.

	x	y	z	U(eq)
U1	109(1)	1514(1)	2077(1)	16(1)
U2	1226(1)	852(1)	2375(1)	12(1)
U3	3067(1)	1807(1)	1230(1)	11(1)
U4	4246(1)	2500	1250	12(1)
S1	20(2)	979(2)	842(3)	27(1)
S2	84(2)	956(2)	4495(3)	29(1)
S3	268(2)	2633(2)	4960(3)	20(1)
S4	301(2)	701(2)	2655(3)	18(1)
S5	480(2)	2672(2)	357(3)	21(1)
S6	716(2)	1515(2)	3262(3)	23(1)
S7	725(2)	6221(2)	379(3)	20(1)
S8	766(2)	3919(2)	2961(3)	31(2)
S9	875(2)	1454(2)	1321(3)	17(1)
S10	922(2)	464(2)	1053(3)	19(1)
S11	1032(2)	631(2)	3900(3)	20(1)
S12	1345(2)	5024(2)	227(3)	16(1)
S13	1555(2)	2554(2)	3672(3)	32(1)
S14	1684(2)	1596(2)	2595(3)	18(1)
S15	1856(2)	926(2)	1253(3)	17(1)
S16	1958(2)	594(2)	3162(3)	16(1)
S17	2012(2)	4751(2)	3479(3)	29(2)
S18	2204(2)	1899(2)	1032(3)	18(1)
S19	2669(2)	1323(2)	2265(3)	19(1)
S20	2873(1)	2504(2)	263(3)	12(1)
S21	2904(2)	1286(2)	26(3)	25(1)
S22	3034(2)	334(2)	651(3)	22(1)
S23	3605(2)	1132(2)	1331(3)	15(1)
S24	3745(2)	3008(2)	211(3)	17(1)
S25	3748(2)	1991(2)	279(3)	20(1)
S26	4633(2)	1740(2)	1388(3)	17(1)
P1	500(2)	948(2)	3689(3)	21(1)
P2	645(2)	991(2)	615(3)	15(1)
P3	2093(2)	1428(2)	1780(3)	14(1)
P4	3332(2)	865(2)	401(3)	16(1)
P5	3459(2)	2514(2)	2732(3)	15(1)
P6	4991(2)	1852(2)	449(3)	14(1)
P7	124(2)	2500	1250	15(2)
Rb1	128(1)	3113(1)	3209(1)	42(1)
Rb2	1784(1)	3694(1)	3109(1)	35(1)
Rb3	3138(1)	428(1)	2467(1)	27(1)
Rb4	4580(1)	694(1)	1166(2)	30(1)
Rb5	1368(1)	2500	1250	52(1)
Rb6	6955(1)	2500	1250	26(1)
Rb7	0	0	1291(3)	98(2)

Acknowledgement

This work was supported by the Deutsche Forschungsgemeinschaft and the Fonds der Chemischen Industrie. We are indebted to Heraeus Quarzschmelze Hanau (Dr. Höfer) for a generous gift of silica tubes, Dr. V. Ksenofontov for collecting the magnetic data, Prof. W. Urland and S. T. Hatscher for discussions, and Dr. M. Kocher for some preliminary investigations.

[1] E. Glatzel, *Ber. Dtsch. Chem. Ges.* **1891**, *24*, 3886 – 3899.
[2] J. Rouxel, in *The Synthesis and Reactivity of Solids*, *Vol. 2* (Ed.: T. T. Mallouk), JAI, London, **1994** pp. 27 – 91.
[3] R. Brec, *Solid State Ionics* **1986**, *22*, 3 – 30.
[4] M. G. Kanatzidis, *Curr. Opin. Solid State Mater. Sci*. **1997**, *2*, 139 – 149.
[5] M. G. Kanatzidis, A. C. Sutorik, *Prog. Inorg. Chem.* **1995**, *43*, 151 – 265.
[6] R. Brec, R. Fréour, G. Ouvrard, J. L. Soubeyroux, J. Rouxel, *Mater. Res. Bull*. **1983**, *18*, 689 – 696.
[7] S. Fiechter, W. F. Kuhs, R. Nitsche, *Acta Crystallogr. Sect. B* **1980**, *36*, 2217 – 2220.
[8] P. Grenouilleau, R. Brec, M. Evain, J. Rouxel, *Rev. Chim. Miner*. **1983**, *20*, 628 – 635.
[9] G. Ouvrard, R. Fréour, R. Brec, J. Rouxel, *Mater. Res. Bull*. **1985**, *20*, 1053 – 1062.
[10] P. Grenouilleau, R. Brec, M. Evain, J. Rouxel, *Rev. Chim. Miner*. **1983**, *20*, 295 – 305; M. Z. Jandali, G. Eulenberger, H. Hahn, *Z. Anorg. Allg. Chem*. **1985**, *530*, 144 – 154.
[11] E. Durand, M. Evain, R. Brec, *J. Solid State Chem*. **1993**, *102*, 146 – 155.
[12] R. Brec, G. Ouvrard, *Solid State Ionics* **1983**, *9 – 10*, 481 – 484.
[13] R. Brec, M. Evain, P. Grenouilleau, J. Rouxel, *Rev. Chim. Miner*. **1983**, *20*, 283 – 294.
[14] M. Evain, R. Brec, G. Ouvrard, J. Rouxel, *Mater. Res. Bull*. **1984**, *19*, 41 – 48.
[15] M. Evain, R. Brec, G. Ouvrard, J. Rouxel, *J. Solid State Chem*. **1985**, *56*, 12 – 20.
[16] C. Wibbelmann, W. Brockner, B. Eisenmann, H. Schäfer, *Z. Naturforsch. Teil A* **1984**, *39*, 190 – 194.
[17] K. Chondrouris, M. G. Kanatzidisr, *Inorg. Chem*. **1998**, *37*, 3792 – 3797.
[18] C. R. Evensen, P. K. Dorhout, *Inorg. Chem.*, in press.
[19] C. R. Evensen, P. K. Dorhout, *Inorg. Chem.*, in press.
[20] G. Gauthier, S. Jobic, R. Brec, J. Rouxel, *Inorg. Chem*. **1998**, *37*, 2332 – 2333.
[21] G. Gauthier, S. Jobic V. Danaire, R. Brec, M. Evain, *Acta Crystallogr. Sect. C*, **2000**, *56*, 117.
[22] K. Chondrouris, M. G. Kanatzidis, *Inorg. Chem*. **2000**, *39*, 1525 – 1533.
[23] J. H. Chen, P. K. Dorhout, *Inorg. Chem*. **1995**, *34*, 5705 – 5706.
[24] J. H. Chen. P. K. Dorhout, J. E. Ostenson, *Inorg. Chem*. **1996**, *36*, 5627 – 5633.
[25] K. Chondroudis, T. McCarthy, M. G. Kanatzidis, *Inorg. Chem*. **1996**, *35*, 840 – 844.
[26] J. Do, J. Kim, S. Lah, H. Yun, *Bull. Korean Chem. Soc*. **1993**, *14*, 678 – 681.
[27] K. Chondroudis, M. G. Kanatzidis, *C. R. Seances Acad. Sci. Ser. B***1996**, *322*, 887 – 894.
[28] a) P. M. Briggs Piccoli, K. D. Abney, J. R. Schoonover, P. K. Dorhout, *Inorg. Chem*. **2000**, *39*, 2970 – 2976; b) R. F. Hess, K. D. Abney, J. L. Burris, H. D. Hochheimer, P. K. Dorhout, *Inorg. Chem*. **2001**, *40*, 2851 – 2859.
[29] K. Chondroudis, M. G. Kanatzidis, *J. Am. Chem. Soc*. **1997**, *119*, 2574 – 2575.
[30] C. Gieck, V. Ksenofontov, P. Gütlich, W. Tremel, *Angew. Chem*. **2001**, *113*, 946 – 948; *Angew. Chem. Int. Ed.* **2001**, *40*, 908 – 911.
[31] M. Evain, M. Queignec, R. Brec, J. Rouxel, *J. Solid State Chem*. **1985**, *56*, 148 – 1587.
[32] V. Derstroff, Ph.D. Dissertation, University of Mainz, Mainz, **1997**.
[33] X. Cieren, J. Angenault, J.-C. Couturier, S. Jaulmes, M. Quarton, F. Robert, *J. Solid State Chem.* **1996**, *121*, 230 – 235.
[34] G. Regelsky, Ph.D. Dissertation, University of Münster, Münster, **2000**.
[35] A. Daoudi, M. Lamire, J. C. Levet, H. Noel, *J. Solid State Chem*. **1996**, *123*, 331 – 336.
[36] W. Suski, *Bull. Acad. Pol. Sci.* **1976**, *24*, 75 – 81.
[37] A. Daoudi, H. Noel, *Inorg. Chim. Acta* **1987**, *140*, 93 – 95.
[38] H. Noel, J. Y. Le Marouille, *J. Solid State Chem*. **1984**, *52*, 197 – 202.
[39] C. Gieck, V. Ksenofontov, P. Gütlich, W. Tremel, unpublished results.
[40] H. Noel, *J. Solid State Chem*. **1984**, *52*, 203 – 210.
[41] R. D. Shannon, *Acta Crystallogr. Sect. A* **1976**, *32*, 751 – 767.
[42] J. M. Tarascon, G. W. Hull, F. J. DiSalvo, *Mater. Res. Bull*. **1984**, *19*, 915 – 923.
[43] K. Chondroudis, M. G. Kanatzidis, *J. Solid State Chem*. **1998**, *136*, 328 – 332.
[44] U. Pätzmann, H. Brockner, *Z. Naturforsch. Teil A* **1983**, *38*, 27 – 36
[45] C. Sourisseau, R. Cavagnat, S. Jobic, R. Brec, *J. Raman Spectrosc*. **1999**, *30*, 721 – 731.
[46] H. Bürger, H. Falius, *Z. Anorg. Allg. Chem*. **1968**, *363*, 24 – 32.
[47] A. J. Freeman, C. Keller, *Handbook on the Physics and Chemistry of the Actinides*, *Vol. 6*, Elsevier, New York, **1991**, pp. 337 – 366.
[48] H. Lueken, *Magnetochemie*, Teubner, Stuttgart, **1999**.

  0947-6539/02/0813-2986 $ 17.50+.50/0

[49] G. K. Wertheim, H. J. Guggenheim, H. J. Levinstein, D. N. E. Buchanan, R. C. Sherwood, *Phys. Rev*, **1968**, *173*, 614–616.
[50] C. Gieck, S. T. Hatscher, W. Urland, W. Tremel, unpublished results.
[51] C. Gieck, F. Rocker, V. Ksenofontov, P. Gütlich, W. Tremel, unpubllished results.
[52] S. Neitzel, Ph.D. Dissertation, University of Mainz, Mainz **1999**.
[53] C. Gieck, F. Rocker, W. Tremel, unpublished results.
[54] SMART, 5th ed., Siemens Analytical X-ray Systems, Inc., Madison, WI, **1998**.
[55] SAINT, 4th ed., Siemens Analytical X-ray Systems, Inc., Madison, WI, **1998**.
[56] G. M. Sheldrick, SADABS, University of Göttingen, Göttingen, **1997**.
[57] G. M. Sheldrick, SHELXTL Plus, Siemens Analytical Instruments, Madison, WI, **1996**; G. M. Sheldrick, SHELXS-86, Program for Crystal Structure Solution, University of Göttingen, Göttingen, **1986**.
[58] G. M. Sheldrick, SHELX-97, Program for Crystal Structure Refinement, University of Göttingen, Göttingen, 1997.
[59] D. T. Cromer, J. T. Waber, *International Tables for X-Ray Crystallography*, *Vol. IV*, Kynoch, Birmingham, (England) **1974**, Tables 2.2A, 2.3.1.
[60] Diamond, Visuelles Informationssystem für Kristallstrukturen, K. Brandenburg, M. Berndt, G. Bergerhoff, University of Bonn, **1998**.
[61] G. Kortüm, *Reflectance Spectroscopy*, Springer, New York, **1969**.
[62] R. J. H. Clarke, *J. Chem. Educ.* **1964**, *41*, 488.
[63] W. W. Wendlandt, H. G. Hecht, *Reflectance Spectroscopy (Chemical Analysis, Vol. 21)*, Interscience, New York, **1966**.
[64] W. Haberditzl, *Magnetochemie*, Akademie Verlag, Berlin, **1968**.

Received: March 15, 2001
Revised: December 12, 2001 [F3133]